

82N12036
19826004163

NASA
TM
81311
c.1

NASA
Technical Memorandum 81311

AVRADCOM
Technical Report 81-A-21



A Pulse-Forming Network for Particle Path Visualization

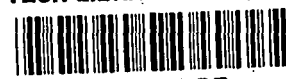
LOAN COPY: RETURN TO
AFWL TECHNICAL LIBRARY
KIRTLAND AFB, N.M.

Kenneth W. McAlister

NOVEMBER 1981



NASA



0150359

NASA

Technical Memorandum 81311

AVRADCOM

Technical Report 81-A-21

A Pulse-Forming Network for Particle Path Visualization

Kenneth W. McAlister

Aeromechanics Laboratory

AVRADCOM Research and Technology Laboratories

Ames Research Center

Moffett Field, California



National Aeronautics
and Space Administration

Scientific and Technical
Information Branch

1981

SYMBOLS

C	capacitance, farad
E	stored electrical energy, J
f	dissipation factor, dimensionless
I	current, A
k	constant in equation (4), dimensionless
L	inductance, H
n	number of LC sections, dimensionless
R	series resistance, Ω
T	pulse duration, sec
U	particle velocity, m/sec
V	charging voltage, V
Z	impedance, Ω

Subscripts

n	network
p	plasma

A PULSE-FORMING NETWORK FOR PARTICLE PATH VISUALIZATION

Kenneth W. McAlister

Ames Research Center
and

Aeromechanics Laboratory, AVRADCOM Research and Technology Laboratories

SUMMARY

A procedure is described for visualizing unsteady fluid flow patterns over a wide velocity range using discrete nonluminous particles. The paramount element responsible for this capability is a pulse-forming network with variable inductance that is used to modulate the discharge of a fixed amount of electrical energy through a xenon flashtube. The selectable duration of the resultant light emission functions as a variable shutter so that particle path images of constant length can be recorded. The particles employed as flow markers are hydrogen bubbles that are generated by electrolysis in a water tunnel. Data are presented which document the characteristics of the electrical circuit and establish the relation of particle velocity to both section inductance and film exposure.

INTRODUCTION

Visual documentation of a simple flow pattern often serves only as collaborating evidence of the phenomenological model postulated based on discrete physical measurements. Many flow fields are of sufficient complexity, however, that visualization must be regarded as essential to the interpretation and presentation of the experimental results. Unsteady flows, which are inherently difficult to comprehend, are also particularly challenging to visualize since (a) they often cannot be observed in real time and (b) their instantaneous streamlines generally cannot be deduced from streak lines (which are relatively easy to produce).

A streak line (or filament line) is defined by the juxtaposition of particles (often too small to resolve) which share a common passage through a given point in space. Since these particles rarely move in tandem when the flow is unsteady, a streak line appears to undergo a continuous deformation and would require a series of "instantaneous" visual recordings to capture the evolution of its shape. As the time rate of distortion increases, the greater is the need for a time-scale expansion of this series of recordings through high-speed cinematography in order to apprehend and later study the phenomenon.

By considering the presence of numerous streak lines in an unsteady flow field and imagining the particles comprising these streak lines to increase sufficiently in size and spacing, a condition is eventually reached where the flow activity that is perceived dissolves from an awareness of each streak line to an awareness of particle paths. This visual transformation to discrete particle tracking is significant because attention is more directly focused on the velocity field. Particle motion in unsteady flow can be visually ascertained either by (a) judicious tracking of discrete particle images

using high-speed cinematography or (b) intentionally blurring (or streaking) discrete particle images using short time exposures. If the intention is to obtain an approximation of the instantaneous velocity field, then either approach may be selected provided that the time and space resolutions are suitably fine. However, if a more qualitative and comprehensive representation of the flow field is preferred, then the latter method should be employed and the time scale relaxed. Such flow visualizations are more convenient to analyze since the time dimension is given a spatial interpretation, thus causing swirling motions, for example, to become readily apparent in a single photograph (see ref. 1).

The length of each segment needed to convey the relative motion of an aggregate of particles is not only subjective, but depends on the scale over which the correlation is being made. Once this length has been determined, it may be regarded as an invariant. With the segment length given, particle velocity then dictates the interval of time (or exposure time) required to record the event. When visualizing the paths of nonluminous particles, this interval is conventionally established either by gating a continuous light source with a light valve (or shutter) or by directly controlling the intrinsic duration of the light source itself.

The gating intervals of mechanical shutters are normally greater than 1 msec and increase considerably with the size of the shutter. Intervals as short as a few nanoseconds can be attained with nonmechanical shutters that employ magnetic or electric fields to alter the optical properties of a medium (ref. 2). Although extremely short shutter speeds are available, it follows from the reciprocity law that as the gating interval decreases, the necessary light flux must increase proportionately. It is usually found that the power demand for the continuous irradiation of nonluminous particles becomes prohibitive as the gating interval decreases; it is therefore more efficient to utilize the megawatt potential of gas ionization as a short-duration light source (ref. 3). In practice, it is normally the particle velocity under study that determines which approach is taken — the interdiction of continuous light or the tailoring of pulsed light.

This study was initiated by the need to visualize and photograph the development of unsteady airfoil separation in a water tunnel for free-stream velocities ranging from 0.3 to 4.9 m/sec. To better identify the presence of a vortical-like structure during boundary-layer breakdown and separation, flow patterns comprised of particle path segments measuring about 5% of the airfoil chord were sought. In order that the recorded images of these segments be independent of free-stream velocity, exposure times from 1 to 16 msec would be required for an airfoil having a 10-cm chord. To establish a point of reference, an exposure test was made using an existing 70-mm camera (shutter limited to 16 msec) and a 1000-W continuous light source (ref. 4). A marginally acceptable exposure was obtained only at the lowest tunnel velocity, and the system was therefore judged to be at least fourfold deficient in brightness for the present study. Based on these shortcomings — limited shutter speed and lack of brightness — the light-interdiction system was abandoned in favor of a high output pulsed light source with controllable duration.

The formation of a light pulse based on the principles of gas ionization is well understood and developed (refs. 3 and 5). The procedure for protracting and shaping a light pulse has also been established (ref. 6) and applied (refs. 7 and 8). Throughout the evolution of strobe technology, emphasis appears to have been placed on obtaining minimum subject blur (ranging from a short-duration pulse for the single frame camera to a long-duration pulse for the high-frame-rate camera). In both extremes, the specific subject velocity and the acceptable image blur are considered as design criteria to be met by the camera and strobe system. In contrast to this more typical situation,

particle path visualization actually depends on intentional and controlled image blurring. Hence the electronic design is governed by two rather uncommon requirements: (1) relatively long gas ionization times and (2) a practical means of varying the duration of the ionization over a wide range. The following discussion describes the application of a modified Guillemin type E pulse-forming network (PFN) meeting these requirements.

During the course of this study, there were numerous occasions when the technical counsel of others provided important guidance and understanding. In particular, discussions with Philip Little, Donald Humphrey, and Larry Russell about electronic theory and design proved especially helpful and are greatly appreciated by the author.

DESCRIPTION OF EQUIPMENT

The primary focus of this experiment was on a pulse-forming network (PFN) used to discharge electrical energy through a xenon flashtube. The PFN consisted of five equal LC sections (fig. 1), with the exception of the first and last section inductances that were increased by 25% to more closely reproduce the classical Guillemin type E pulse shape (ref. 6). All five capacitors were $70\text{ }\mu\text{F}$ and rated at 5 kV. A total of 25 inductors were constructed, giving 5 inductors of equal value at each of five distinct levels of inductance: 100, 400, 1,600, 6,400, and 25,600 μH . Since each level was a factor of 4 larger than the next lower level, the 25% increase in inductance needed for the end sections could be conveniently obtained by series patching with an inductor from a lower level set (the obvious exception being for the 100- μH PFN). The 5 equal-valued inductors comprising a set were oriented along a common axis and spaced to give a mutual inductance equal to approximately 15% of the self-inductance (ref. 6).

The light source was an EG&G FXG-77C-12C linear water-cooled xenon flashtube. The gas volume measured 30 cm in length and 2 cm in diameter. The maximum input rating for the flashtube was 15,100 J for a 1-msec duration flash. Initial ionization of the flashtube was established

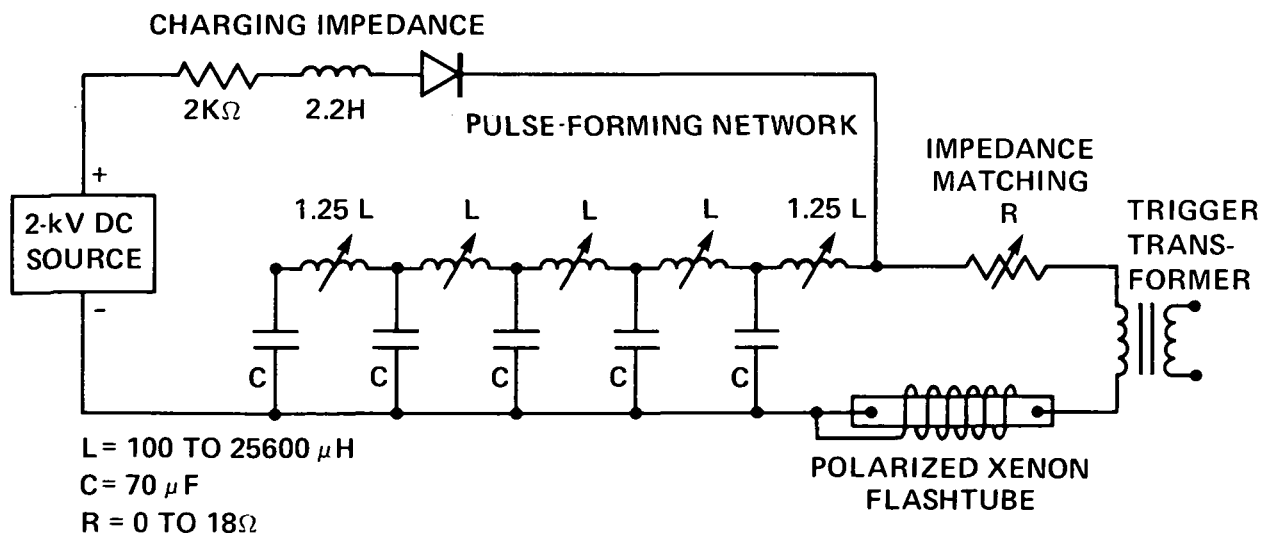


Figure 1.— Modified Guillemin type E circuit used to obtain variable light pulse intervals.

with a series trigger using a transformer with a $0.5 \mu\text{sec}$ rise time and a saturation inductance of $100 \mu\text{H}$. The trigger wire (enveloping the flashtube-water jacket), supplied by the manufacturer for the purpose of external triggering, was instead connected to the negative electrode to extend the reference plane around the gas. The operating voltage for the circuit was maintained at 2 kV throughout the experiment. The impedance-matching resistance shown in figure 1 was comprised of low-inductance, $1\text{-}\Omega$ resistors patched in parallel and in series to obtain resistance values up to 18Ω .

Light measurements were made with a silicon-photovoltaic detector-probe that was uniformly sensitive over the visible and near infrared spectrum. A $50\text{-}\Omega$ resistor was placed across the photodiode to enable oscilloscope measurements of the light pulse shapes to be made. The response time of the detector was approximately $0.2 \mu\text{sec}$. Total received-light measurements were made using a pulse-integrating attachment. Light-related pulses as well as voltage pulses at various points in the circuit were recorded and analyzed using a transient-signal capturing instrument.

The example photograph of particle path visualization was obtained in the Aeromechanics Water Tunnel Facility at Ames Research Center. The hydrogen bubbles generated by continuous electrolysis provided the minute flow markers that were illuminated by the flashtube and photographed. These bubbles are produced at platinum electrodes exposed to the electrolyte along the upper surface of the nonconducting model. The trajectory of each bubble is assumed to represent the motion of the fluid that it displaces, so the collective activity of the bubbles over a finite period of time can be used to study the kinematic state of the viscous domain surrounding the model.

DEVELOPMENT OF EQUATIONS

The following discussion assumes that film images are to be formed from the light reflected from discrete nonluminous particles that are moving with a fluid. Expressions are presented which describe the generation of this light based on the photoemission characteristics of a xenon flashtube and the discharge of electrical energy from a pulse-forming network. A procedure is discussed for adjusting the network to produce a constant image length for any given particle velocity. In addition, a relation is developed for determining the corresponding film exposure.

The effect of discharging energy from a pulse-forming network in place of a simple inductor-capacitor section is demonstrated in figure 2. Both circuits have the same total capacitance (therefore the same quantity of available energy) and the same total inductance, yet the time histories are quite different. The pulse-forming network clearly offers the advantage of a more definable pulse interval as well as a more uniform emission of light from the flashtube. The shape-squaring characteristic derived from the five or more LC sections defining the PFN is well known from early radar theory (ref. 6) and has since been applied to the shaping of light pulses. The present study is concerned with devising a convenient and systematic method for modifying the pulse width from the PFN.

Consider the current pulse duration, T , delivered by a PFN:

$$T = 2\sqrt{L_n C_n} = 2n\sqrt{LC} \quad (1)$$

where the subscript n denotes the total network value that accrues from all contributing section

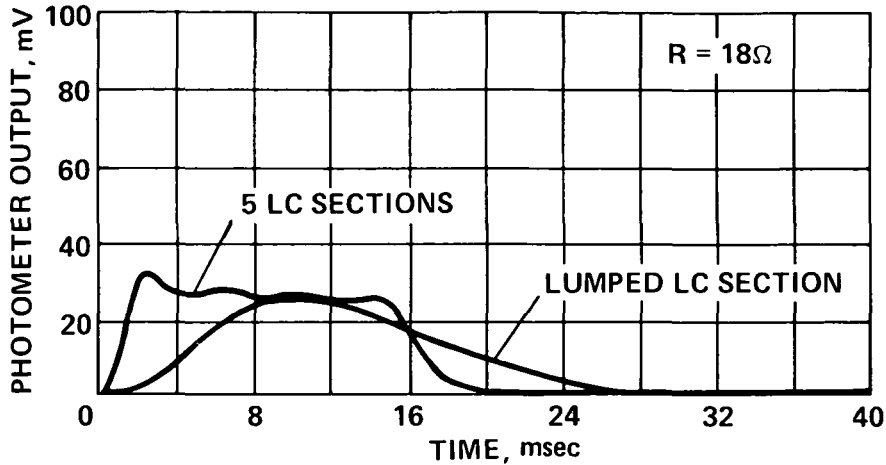


Figure 2.— Shaping of light pulse using a modified Guillemin type E discharge circuit (results for 26,000 μH PFN).

values (without subscript). Three approaches to varying the pulse duration are available: (1) by changing the number of LC sections, n , (2) by changing the value of L or C (or both) for a fixed number of sections, and (3) by employing a fixed PFN designed to give the longest desired duration, but clipping the pulse before completion by short-circuiting the network (ref. 8). Although arguments can be given in favor of each approach, a decision based on cost and convenience was made to vary the network inductance.

The length of the visualized particle path is determined by the particle velocity, U , and the light-pulse duration, T , according to

$$\text{Film-image length} \sim 2U\sqrt{L_n C_n} \quad (2)$$

For fixed capacitance, a 1:16 range of particle velocities would require a corresponding 256:1 range of network inductances to enable constant image lengths to be recorded. Based on the following parameters: (1) particle path segments were to be 5% of the airfoil chord in all cases, (2) the airfoil chord measured 10 cm, (3) the highest particle velocity would be 4.9 m/sec, and (4) the fact that 70- μF capacitors had already been acquired based on preliminary exposure estimates, it was determined that the smallest section inductance would have to be 100 μH . Since this value of inductance corresponded to the maximum particle velocity, the minimum particle velocity would require a section inductance of 25,600 μH . Thus a PFN was defined and assembled for each level of a four-fold increase in particle velocity (1, 2, 4, 8, and 16 times).

Assuming such factors as light-path transmittance and particle reflectance to be invariant, the exposure of the film by the image of a moving particle can be expressed as

$$\text{film exposure} \sim \frac{(\text{light flux})(\text{lens aperture})}{\text{particle velocity}} \quad (3)$$

The light output resulting from photoionization is proportional to the ionization current according to

$$\text{light flux} \sim (\text{ionization current})^k \quad (4)$$

where the exponent generally appears to range over $1 < k < 2$ and approaches the upper limit as the current density (based on plasma cross-sectional area) increases (refs. 7 and 8). To determine the range of lens apertures needed to yield the same image exposure (and film density) over a 16:1 span of particle velocities, an expression is needed for the ionization current. This quantity can be derived by first considering the total electrical energy stored in the network:

$$E = \frac{1}{2} C_n V^2 \quad (5)$$

Recall that C_n represents the network capacitance and is equal to the contribution of all section capacitors, $C_n = nC$. The ionization current can be calculated from the charging voltage and the circuit "resistance" according to

$$I = \frac{V}{Z_n + Z_p + R} \quad (6)$$

where Z_n and Z_p are network and plasma impedances, respectively, and R is the series resistance added to inhibit current reflections due to improper impedance matching between the network and the flashtube. Although maximum power is transferred from the network when the circuit is critically damped ($Z_n = Z_p + R$), it should be noted that maximum current (which determines maximum light output) occurs when the circuit resistance ($Z_n + Z_p + R$) is minimized.

The plasma impedance is known to vary inversely with the square root of the current density (ref. 9); for the xenon flashtube used in this study (and assuming that the plasma fills the tube), the impedance is given by

$$Z_p = \frac{20.5}{\sqrt{I}} \Omega \quad (7)$$

(with I expressed in amps). The network impedance is given by

$$Z_n = \sqrt{L_n/C_n} \quad (8)$$

Equations (6) and (8) may be combined and rearranged to yield the following expression for the ionization current:

$$I = \frac{4(1/2 C_n V^2) f}{2\sqrt{L_n C_n} V} \quad (9)$$

where f is herein defined as a dissipation factor:

$$f = \frac{Z_n}{Z_n + Z_p + R} \quad (10)$$

which assumes values of $0 < f < 1$ and is equal to $1/2$ for a critically damped circuit. In this form, the ionization current can be readily given the following physical description which more directly reflects the dynamic behavior of the discharge circuit:

$$\text{ionization current} = \frac{4 (\text{stored energy}) (\text{dissipation factor})}{(\text{pulse duration})(\text{charging voltage})} \quad (11)$$

Combining equations (3), (4), and (9) yields the following expression for the film exposure:

$$\text{film exposure} \sim \frac{\text{lens aperture}}{\text{particle velocity}} (Vf\sqrt{c/L})^k \quad (12)$$

Taking the charging voltage and the section capacitance to be constant, and assuming for the moment that $f = 1$ and $k = 2$, an estimate of exposure can be made. In equation (2), for a fixed image length and a given number of LC sections, the particle velocity and section inductance must conform to $U\sqrt{L} = \text{constant}$. This would therefore imply that, for a 256:1 range of inductances, a corresponding 16:1 aperture range would be required. Hence a fourfold variation in exposure (or four lens f-stops) must be anticipated, and a trial exposure to establish maximum allowable depth of field (minimum aperture) should be made at the minimum particle velocity condition. If it is found that insufficient film density results even at maximum aperture, then the charging voltage must be increased. If, at the other extreme, an excessive amount of film density results, either an appropriate neutral-density filter can be used or the charging voltage decreased. In neither case should the section capacitance be changed since this would result in a change in the image length.

RESULTS OF EXPERIMENT

The purpose of this section is to demonstrate the validity of the governing equations, to indicate the optimum operating conditions of the circuit, and to present an example of a particle path visualization. Instantaneous photometric histories were recorded for each network and measurements of the resulting pulse interval were made at a level equal to 1/3 the pulse plateau. The pulse intervals for the five networks were found to vary linearly with the square root of the section inductance (fig. 3) and quantitatively agree with theory, except that the coefficient in the equation describing the experimental results is about 10% higher than would have been predicted using equation (1). Although experimental uncertainty may be partially responsible for this difference, it is believed to be primarily due to the fractional value of the plateau used to determine the pulse interval. Equation (1) is based on a level equal to 1/2 the plateau (ref. 10), whereas the experimental results were based on 1/3 the plateau because it was judged to be more representative of film sensitivity thresholds. In either case, since the light pulse interval required to produce a particle path image of given length is inversely proportional to the velocity of the particle, it follows that

$$U\sqrt{L} = \text{constant} \quad (13)$$

which is consistent with the discussion of equation (2) in the previous section.

Maximum power is transferred from the pulse-forming network when its impedance is matched by that of the flashtube. However, since the network inductance is to be greatly varied to obtain the required pulse-interval range, the network and flashtube impedances will normally be substantially unmatched. To illustrate the consequence of unmatched impedances, consider the network defined by $L = 25,600 \mu\text{H}$. According to equation (8), the network impedance would be 20Ω . If the load impedance were matched to this value and the charging voltage set at 2000 V, then the

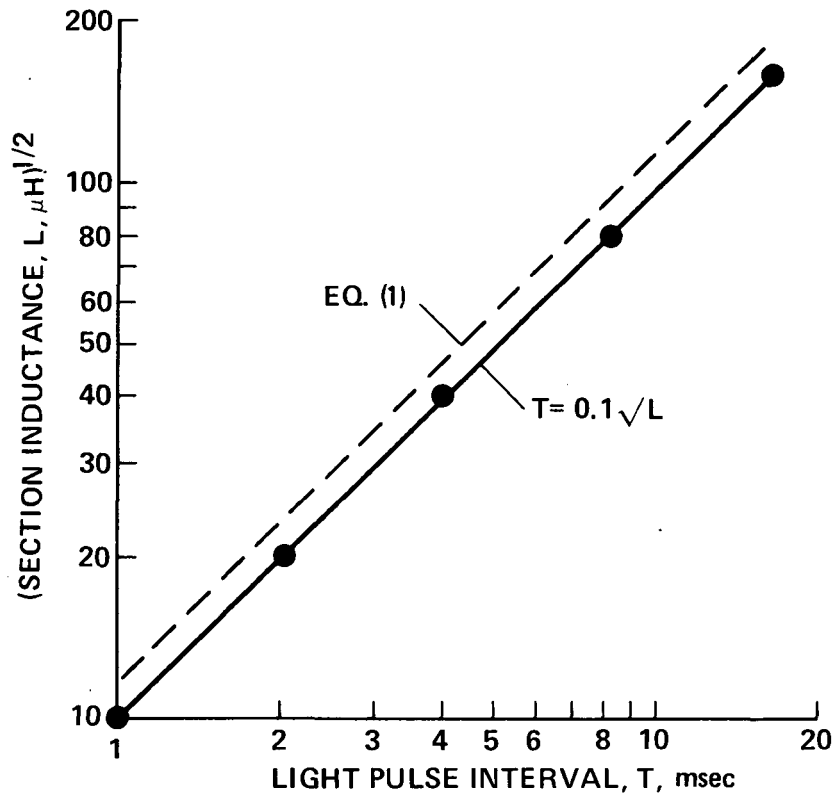


Figure 3.— Section inductance required to obtain a given light pulse interval (based on 1/3 pulse plateau).

peak current would be 50 amps. Substituting this value of peak current into equation (7) yields an estimate for the flashtube impedance of 3Ω . The network and flashtube impedances are clearly unmatched and, unless this difference is eliminated by placing a resistor equal to 17Ω in series with the flashtube, the circuit may oscillate. Circuit oscillations must be avoided since they not only produce multiple flashes, but can cause electrode damage in a polarized flashtube during current reversals. Although the need for a small amount of impedance-matching resistance may be expected in practice, a large amount (as calculated above) would be undesirable since it would consume a correspondingly large amount of available energy from the network. The impact of this added load resistance on flashtube performance is shown in figure 4. When properly matched, a well-shaped pulse results. As the value of the resistor is reduced, the mean amplitude increases and the slope of the plateau steepens. The extreme case with no added resistance provides an example of a secondary flash that resulted from a negative voltage swing across the flashtube. The role of the impedance-matching resistor is therefore seen to be (a) to level the pulse plateau and (b) to prevent current reflections. If plateau leveling were not a consideration, a diode could be used in place of the resistor to directly block a current reversal. This would be an efficient remedy if total light energy were the only factor (fig. 5). However, assuming that some degree of plateau leveling is desired, it is fortunate that the network does not have to be exactly matched to prevent a current reversal. Indeed, tests of all five networks revealed that the circuit may be considerably underdamped without any measurable secondary flash (fig. 6). This behavior is believed to be due to the characteristic holdoff voltage as well as the ionization properties of the flashtube at the completion of the primary current pulse. A special case also appears in figure 6 and is labeled as "lumped LC." In this case, the elements of the 25,600- μ H PFN were reassembled into a single LC section to extend the comparison shown in figure 2. Integrated light measurements show that the PFN results in a greater conversion to light energy than in the lumped element case, thereby suggesting a nonlinear

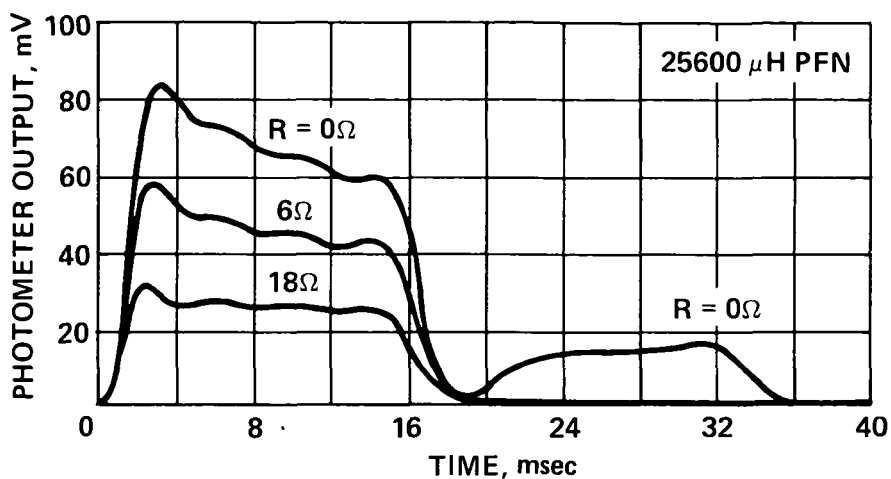


Figure 4.— Importance of impedance matching resistor on suppression of secondary pulse and squaring of primary pulse.

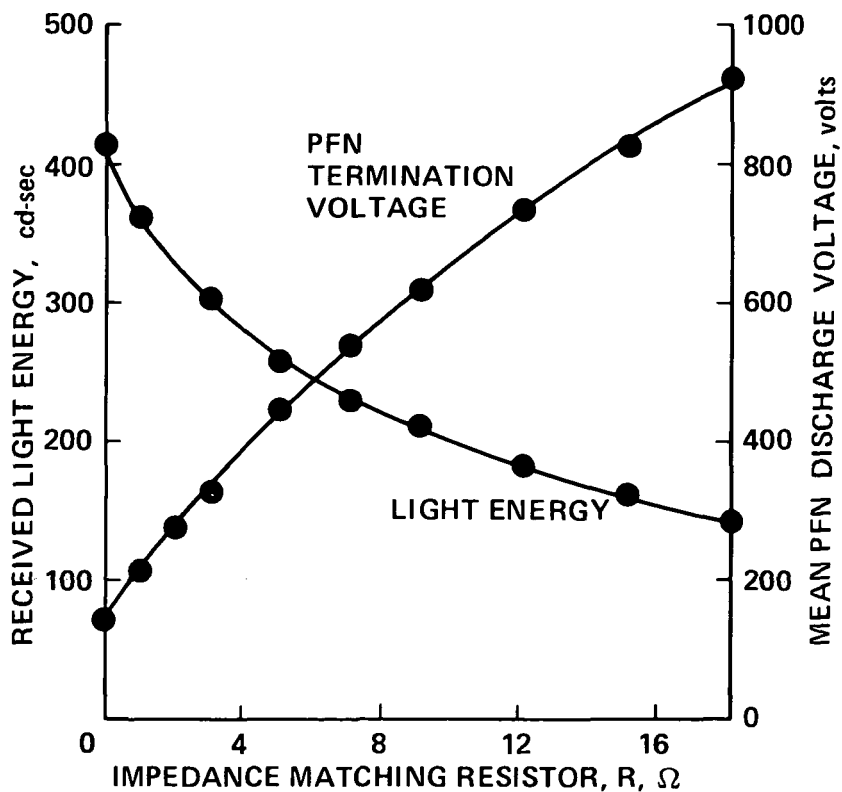


Figure 5.— Effect of impedance matching resistor on integrated light output and mean network voltage for 25,600 μ H PFN.

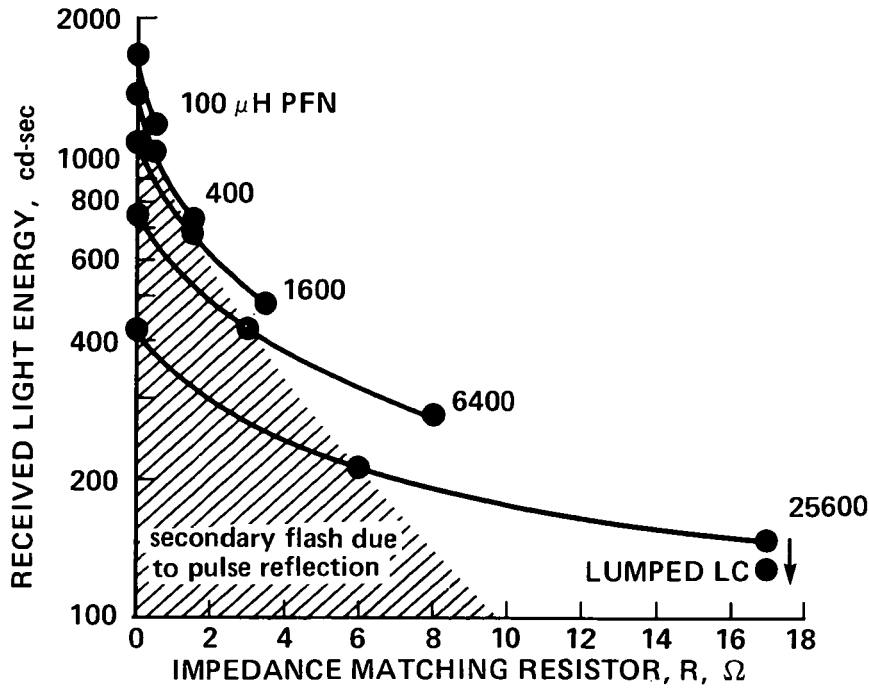


Figure 6.— Effect of pulse-forming network on integrated light output.

dependence on current and the significance of maintaining a high level of current during the discharge.

A significant unknown remaining to be resolved is the factor k , which appears as an exponent in equation (4) and describes the dependence of light flux on ionization current. For any given PFN, the pulse duration (for the primary pulse in the case of reflections) was found to be essentially independent of the size of the impedance-matching resistor. Therefore, several values of resistance were used with each PFN to obtain current and light flux data at each pulse-duration level. The current was derived from the mean plateau voltage measured across the resistor in use. The light flux was derived from the integrated light measurement and the corresponding pulse width. The results for three measurements made for each of the five networks are shown in figure 7. The data appear to be well approximated in the logarithmic plane by a single straight line given by

$$\text{light flux} = 15.5 (\text{current})^{1.68} \quad (14)$$

(where the current is in amps and the resulting light flux is in candela).

An estimate can now be given for the variation in aperture required to yield a constant film density over the range of pulse durations. As stated before, the particle velocity varies inversely with the light-pulse duration required to produce an image of constant length; hence, equation (12) can be written

$$(\text{lens aperture}) (\text{pulse duration}) (f/\sqrt{L})^{1.68} = \text{constant} \quad (15)$$

Considering the two extreme networks, the following table of values can be calculated:

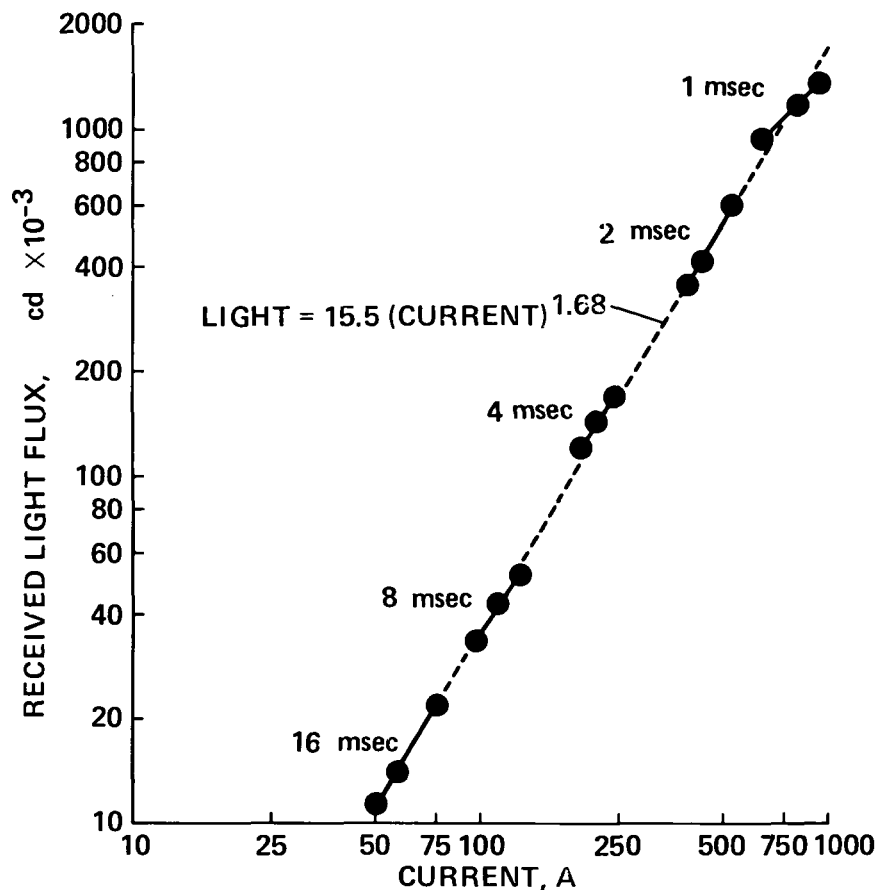


Figure 7.— Instantaneous light generated by current at five pulse-interval levels.

Substituting the appropriate values into equation (15) shows that the lens aperture for the 16-msec network must be a factor of 9 times larger than that for the 1-msec case. To test the validity of this calculation, film was exposed over a range of aperture settings using an 18% reflectance surface as the subject area. Based on densitometer measurements of the resulting negatives, it was found that the 16-msec network required a three-stop increase in aperture to equal the density produced by the 1-msec network. Since a three-stop increase is equivalent to a factor of 8, the formulations were judged to be suitably accurate. The recommended values for resistance and aperture for the five networks are as shown in table 2. Based on a 10-cm chord model, the range of particle velocities given in the first column corresponds to a Reynolds number range from 30,000 to 500,000 in water.

TABLE 1.— CIRCUIT CONDITIONS AT TWO EXTREMES

PFN, μH	T , msec	R , Ω	I , amp	Z_p , Ω	f
100	1	0	1000	0.2	0.85
25,600	16	6	58	2.7	.70

Based on densitometer measurements of the resulting negatives, it was found that the 16-msec network required a three-stop increase in aperture to equal the density produced by the 1-msec network. Since a three-stop increase is equivalent to a factor of 8, the formulations were judged to be suitably accurate. The recommended values for resistance and aperture for the five networks are as shown in table 2. Based on a 10-cm chord model, the range of particle velocities given in the first column corresponds to a Reynolds number range from 30,000 to 500,000 in water.

To illustrate the importance of particle path visualization and to demonstrate the applicability of the pulse-forming network for this purpose, fluid flow around an airfoil section was established at a free-stream velocity of 0.6 m/sec (corresponding to a Reynolds number of 60,000). The airfoil was given a sinusoidal pitching motion of sufficiently high amplitude to cause flow separation over the upper surface. The high transient loads commonly associated with unsteady separation were

TABLE 2.— NETWORK PERFORMANCE

U , msec	PFN, μ H	R , Ω	T , msec	Aperture
4.9	100	0	1	reference
2.5	400	0.5	2	+3/4 stop
1.2	1,600	1.5	4	+1-1/2
.6	6,400	3.0	8	+2-1/4
.3	25,600	6.0	16	+3

believed to be due to the formation and passage of a vortex over the airfoil. To verify the presence of such a vortex, some degree of intentional image blurring using discrete flow markers (such as hydrogen bubbles) would be needed to produce particle path segments of finite length, thereby revealing the rotational quality of any vortical motion that might exist. For this purpose, hydrogen bubbles were generated on

the surface of the airfoil and were carried away by the fluid comprising the separated flow domain. To determine the required exposure time, it was assumed that the free-stream velocity would be representative of the velocity of the bubbles carried into the separated region. Referring to table 2, a 4-m/sec particle velocity corresponds to an exposure time of 8 msec. Figure 8 is a photograph taken at 8 msec (producing the desired particle path segments) as well as one taken at 1 msec (producing a "frozen-flow" image). While the frozen-flow image yields a more accurate presentation of the instantaneous separated flow domain, only the "correctly" exposed image reveals the large scale motion of the fluid needed to identify any rotational activity. If, for example, the same flow environment were to have been examined at a velocity of 4.9 m/sec, then the 1-msec exposure would have been the "correct" time and the 8-msec exposure too long. In this case, a long exposure may be difficult to interpret because of image overlays due to the convection of the vortex through the fixed field of view.

CONCLUSIONS

A pulse-forming network with variable inductance can be used to produce well-modulated light pulses over a wide range of pulse durations. The network and flashtube impedances can be greatly mismatched without current reversal to attain a compromise between optimum pulse squaring and maximum ionization. Simple relations can be used to determine the correct section inductance and film exposure based on a given particle velocity.

Ames Research Center

National Aeronautics and Space Administration

and

Aeromechanics Laboratory

AVRADCOM Research and Technology Laboratories

Moffett Field, Calif. 94035, July 27, 1981



Figure 8.— Comparison between “frozen flow” (1 msec) and particle path (8 msec) visualizations of unsteady airfoil separation.

REFERENCES

1. Werlé, H.: Hydrodynamic Flow Visualization. Annual Review of Fluid Mechanics, vol. 5, 1973, pp. 361-382.
2. Hyzer, W. G.: Engineering and Scientific High-Speed Photography. The Macmillan Co., 1962.
3. Edgerton, H. E.: Electronic Flash, Strobe. McGraw-Hill Book Co., 1970.
4. McAlister, K. W.; and Carr, L. W.: Water-Tunnel Experiments on an Oscillating Airfoil at $Re = 21,000$. NASA TM-78,446, 1977.
5. Marr, G. V.: Photoionization Processes in Gases. Academic Press Inc., 1967.
6. Glasoe, G. N.; and Lebacqz, J. V.: Pulse Generators. M.I.T. Radiation Laboratory Series, Boston Technical Publishers, Inc., 1964.
7. Thackery, D. P. C.: Control of the Acting Emission of Electronic Discharges. Proceedings of the 3rd International Congress on High Speed Photography, London, England, Sept. 1956, pp. 21-29.
8. Krehl, P.: A High-Intensity Point Light Source with Adjustable Light Duration. Proceedings of the 12th International Congress on High Speed Photography, Toronto, Canada, Aug. 1976, pp. 468-475.
9. Goncz, J. H.: New Developments in Electronic Flashtubes. ISA Transactions, vol. 5, no. 1, Jan. 1966, pp. 28-36.
10. Graf, R. F.: Electronic Design Data Book. Van Nostrand Reinhold Co., 1971.

1. Report No. NASA TM-81311 AVRADCOM TR 81-A-21		2. Government Accession No.		3. Recipient's Catalog No.	
4. Title and Subtitle A PULSE-FORMING NETWORK FOR PARTICLE PATH VISUALIZATION				5. Report Date November 1981	
				6. Performing Organization Code	
7. Author(s) Kenneth W. McAlister				8. Performing Organization Report No. A-8671	
9. Performing Organization Name and Address NASA Ames Research Center and Aeromechanics Laboratory AVRADCOM Research and Technology Laboratories Moffett Field, CA 94035				10. Work Unit No. 992-21-01	
				11. Contract or Grant No.	
12. Sponsoring Agency Name and Address National Aeronautics and Space Administration Washington, DC 20546 and U.S. Army Aviation Research and Development Command St. Louis, MO 63166				13. Type of Report and Period Covered Technical Memorandum	
				14. Sponsoring Agency Code	
15. Supplementary Notes Kenneth W. McAlister: Aeromechanics Laboratory, AVRADCOM Research and Technology Laboratories.					
16. Abstract A procedure is described for visualizing nonsteady fluid flow patterns over a wide velocity range using discrete nonluminous particles. The paramount element responsible for this capability is a pulse-forming network with variable inductance that is used to modulate the discharge of a fixed amount of electrical energy through a xenon flashtube. The selectable duration of the resultant light emission functions as a variable shutter so that particle path images of constant length can be recorded. The particles employed as flow markers are hydrogen bubbles that are generated by electrolysis in a water tunnel. Data are presented which document the characteristics of the electrical circuit and establish the relation of particle velocity to both section inductance and film exposure.					
17. Key Words (Suggested by Author(s)) Streakline visualization Unsteady flow			18. Distribution Statement Unclassified - Unlimited STAR Category - 02		
19. Security Classif. (of this report) Unclassified	20. Security Classif. (of this page) Unclassified		21. No. of Pages 18	22. Price* A02	

National Aeronautics and
Space Administration

SPECIAL FOURTH CLASS MAIL
BOOK

Postage and Fees Paid
National Aeronautics and
Space Administration
NASA-451



Washington, D.C.
20546

Official Business

Penalty for Private Use, \$300

3 1 10, A, 111281 S00903DS
DEPT OF THE AIR FORCE
AF WEAPONS LABORATORY
ATTN: TECHNICAL LIBRARY (SUL)
KIRTLAND AFB NM 87117

NASA

POSTMASTER: If Undeliverable (Section 158
Postal Manual) Do Not Return
